Experimental und numerical investigations on cooling efficiency in the secondary cooling zone during continuous casting of steel

G. Arth, M. Taferner, C. Bernhard, Chair of Ferrous Metallurgy, Montanuniversität Leoben, Austria

G. Arth, Chair of Ferrous Metallurgy, Montanuniversität Leoben, Franz-Josef-Straße 18, A-8700 Leoben, Austria. Tel.: +43-3842-402-2237, Fax: +43-3842-402-2202, email: gregor.arth@unileoben.ac.at

Abstract
Cooling strategies in continuous casting of steel can vary from rapid cooling to slow cooling, mainly controlled by adjusting the amount of water sprayed onto the surface of the product. Inadequate adjustment however can lead to local surface undercooling or reheating, leading to surface and inner defects.
This paper focuses on secondary cooling during continuous casting of steel and the experimental and numerical prediction of surface temperature distributions over the product width. The first part of this publication explains the determination of heat transfer coefficients (HTC) on laboratory scale, using a so called nozzle measuring stand (NMS) at the Chair of Ferrous Metallurgy (CoFM), Montanuniversitaet Leoben (MUL). Based on measured water distributions and determined HTC's for air-mist nozzles using the NMS, surface temperatures are calculated by a transient 2D-model for a steel plate moving at constant velocity, explained in the second part of this paper. Simulations are carried out varying water impact density and spray water distribution, consequently influencing the local HTC distribution over the product width. Furthermore, these results will be interpreted with regard to their consequence for surface and internal quality of the cast product. The results reveal the difficulty of correct adjustment of the amount of sprayed water, concurrent influencing water distribution and thus changing HTC distribution and surface temperature, as will be shown in the end of this publication.

Key Words
Continuous casting, secondary cooling, heat transfer coefficients, measurement, simulation, product quality

Introduction

Secondary cooling strategies of continuous casting processes can vary from rapid to slow cooling. Water or air-mist nozzles with a wide range of possible spray water distributions and/or impact densities aim on uniform heat removal during the casting process. Even if high effort is done in research in homogeneous water distribution over a wide range of operation parameters (varying water flow rate, air pressure e.g.) [1], resulting heat transfer coefficients (HTC) can still differ over spray width, leading to uneven heat removal during casting. [2,3]
Current simulations typically use mean heat transfer coefficients based on adjusted water impact densities as input for calculation of continuous casting processes, neglecting inhomogeneous water distributions of spray width, but for simplicity and calculation speed. However, different researchers [2–10] illustrate parameters like spray water temperature, water/air ratios, casting speed and more as important influence factors on heat removal. Regarding these facts, the demand on more detailed information on heat removal lead to the development of several test assemblies on laboratory scale to measure local heat transfer coeffients. [7,11–13]

Experimental equipment

A so called nozzle-measuring-stand (NMS) at the Chair of Ferrous Metallurgy (CoFM), Montanuniversität Leoben (MUL) - developed as prototype within the frame of a K1-MET-Phase1-project in cooperation with voestalpine Stahl Donawitz GmbH - is used to determine local HTC's with the option on variation of a number of nozzle- and casting parameters.
Figure 1 presents a schematic drawing of the HTC measurement set-up. The NMS can be separated into 3 levels:

- Level 1 contains a cylindrical steel sample, the induction heating unit and the sample support stand (positioning unit on linear axes)
- Level 2 is called the "wet-zone", where the spray nozzles are fixed in definite positions, spraying upwards for HTC measurements and spraying downwards, to measure water distribution.
- Level 3 stores technical equipment like air and water supply and the cooling unit of the induction device.

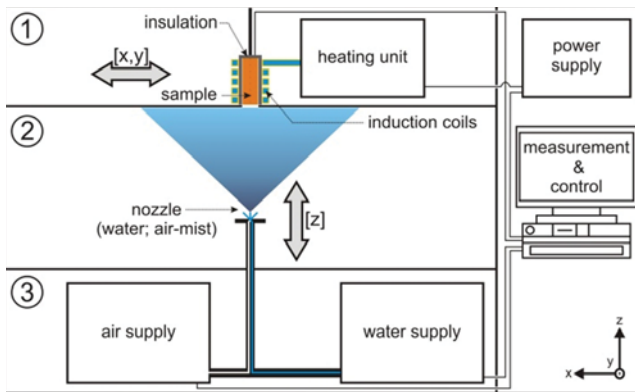The current set-up of the NMS is shown in Figure 2.

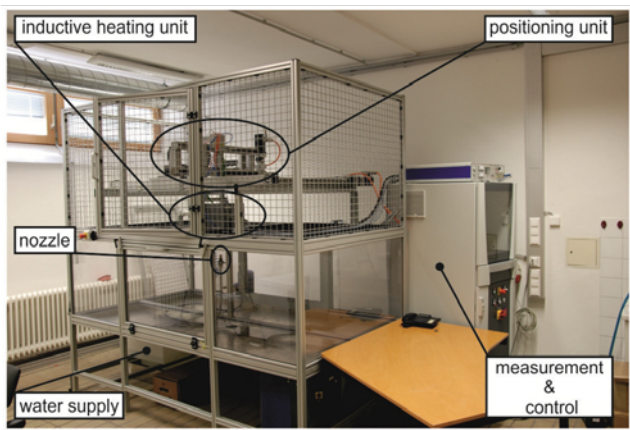*Figure 1: NMS build-up at the CoFM to determine local HTC.*

Figure 2: Current set up of the NMS at the CoFM, Montanuniversität Leoben.

Determination of HTC

HTC's measurements are carried out using a cylindrical sample made of scale resisting austenitic steel (1.4841) with diameter to height ratio of 1:1.8. Three thermocouples are positioned along the center axis of the steel sample at different distances to the cooled steel surface (bottom of the sample), where an additional thermocouple is fixed. The lateral and the top of the steel surface are insulated to ensure one-dimensional heat flow towards the bottom during cooling.

Figure 3 displays the principle to characterize a flat fan nozzle regarding HTC:

   i.   The first HTC measurement typically starts at the center of the nozzle. The sample is positioned at a certain distance to the water spray to ensure no contact between water and steel during heating.
   ii. Heating of the cylindrical steel sample to the aimed surface temperature (T_{max} = 1100°C) is done by inductive heating under normal atmosphere.
   iii. When reaching constant volumetric flow of water (or water-air mixture), inductive heating is switched off and the sample is moved at constant velocity (casting speed) through the water spray ("a" in Figure 3).

   iv. Temperatures are measured inside the steel sample during this movement using type S or type K thermocouples, depending on the desired maximum surface temperature.
   v.   After this first measurement the water (water-air mixture) is switched off and the steel sample is moved to the next position (C+1/5L in Figure 3), starting again at step "ii".

Local HTC are computed by inverse calculation of measured temperatures (see also Figure 4) inside the steel sample.
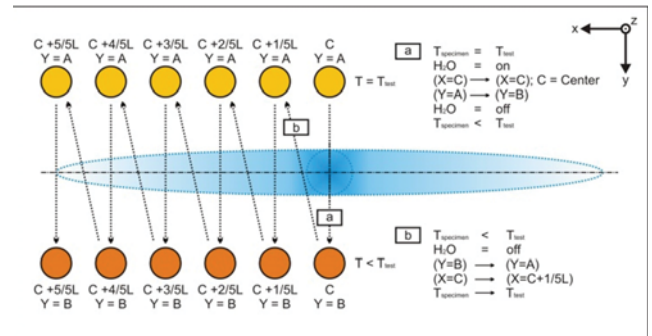

Figure 3: Scheme of nozzle characterization of a flat fan nozzle by the NMS; No variation of temperature, velocity or water impact density.
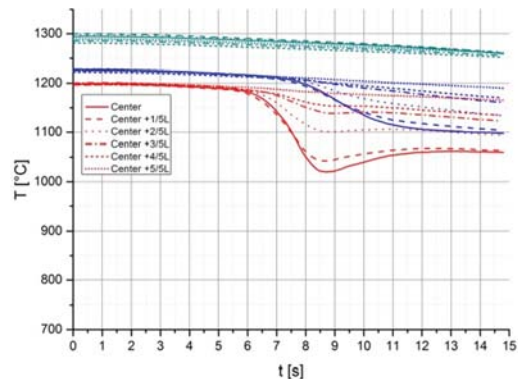

Figure 4: Examples for temperature progressions of Tc1 – Tc3 during HTC measurement (see Figure 3); results not presented in this publication.

Determination of water distribution

Water distribution is likewise measured using the NMS, but contrary to the HTC measuring set up, the nozzle is fixed at the top of level 2 with water exit direction downwards. A self-designed patternator, consisting of 7 single transparent columns, with each column comprising of 100 single 10x10x380mm (LxWxH) cups, is placed at the bottom of the set-up for water distribution measurement, depicted in Figure 5. Figure 6 presents an image taken during a spray water distribution measurement with the self-designed patternator inside the NMS.

The nozzle is fixed at a definite distance to the top of the columns (distance to slab e.g.). After reaching a

constant volumetric flow of water (l/min) and air pressure (bar), the columns are placed side by side at the bottom of level 2 for a certain time, mainly depending on the adjusted water flow rate. The patternator is removed, divided into 7 columns and an image is taken of each column by a commercially available reflex camera. Using digital image processing the amount of water in every single cup is measured. Combining the time of measurement with the amount of collected water, the water distribution of a water or air-mist nozzle can be standardized and compared for different parameter variations. A Matlab routine written in-house is used to visualize the water distribution, examples will be presented later in this publication.
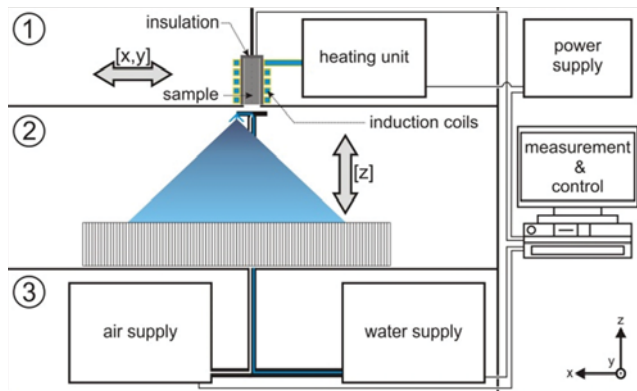

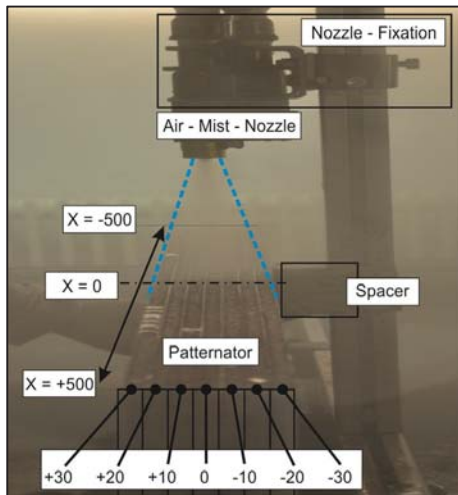*Figure 5: NMS build-up at the CoFM to measure spray water distribution.*

Figure 6: Current set up of the NMS to measure spray water distribution (compare Figure 5).

Results

Both investigated nozzles are typically used in parallel arrangement in a conventional slab casting machine. Table 1 presents the test schedule with measurement parameters; layout and mounting information can be taken out of Table 2 and Figure 7. HTC measurements were carried out for combinations of minimum water flow rate at minimum air pressure (further stated as "case a"), and

maximum water flow rate and maximum air pressure ("case b") for each nozzle. Measured water distributions are depicted in Figure 8 and Figure 9.

Nozzle	H_2O_{max}	H_2O_{min}	Air_{max}	Air_{min}	$T_{surf.}$	v_{cast}
	[l/min]	[l/min]	[bar]	[bar]	[°C]	[m/min]
A	7	3.0			1100	
B	3.5	1.5	2.5	1.1	900	0.8

Table 1: Test schedule for HTC and water distribution measurements.

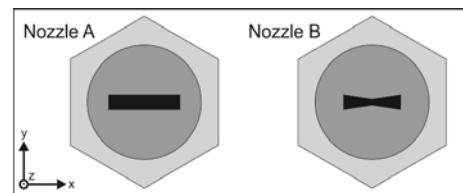| Nozzle	Spray Angle	Distance to surface
	[°]	[mm]
A	90	396
B	60	346

Table 2: Nozzle layout and mounting.

Figure 7: Schematic outlet appearance of nozzle A and nozzle B.

The water distribution was standardized for all measurements, whereas the maximum amount of water in one cup was taken as 100%, all others were scaled in this respect. Images in Figure 9 are printed in falsified aspect ratio for a better viewability of the water distribution in Y-direction. Spray water distributions of both nozzles can be summarized as follows:

- Nozzle A owns a pyramidal, rectangular spray water distribution with the highest amount of water at the center of the nozzle.
- Contrary to nozzle A, two maxima are located at the edge (X-orientation) of nozzle B.
- The higher the amount of water and air pressure (case "b"), the more distinct the appearance at both nozzles.
- No entire symmetric water distribution is observed, neither for nozzle A or B.
- The limited patternator dimension in Y-direction leads to an incomplete imaging of the spray water distribution in all cases.

Even if the patternator limitation in Y-direction leads to information losses, the small cup dimensions of 10x10mm provide a high resolution rate and localized water maxima can be detected very accurate. Knowing this localized maxima and minima helps the selection of the further HTC measurement positions, as can be seen in Figure 9, drawn as grey dotted lines.
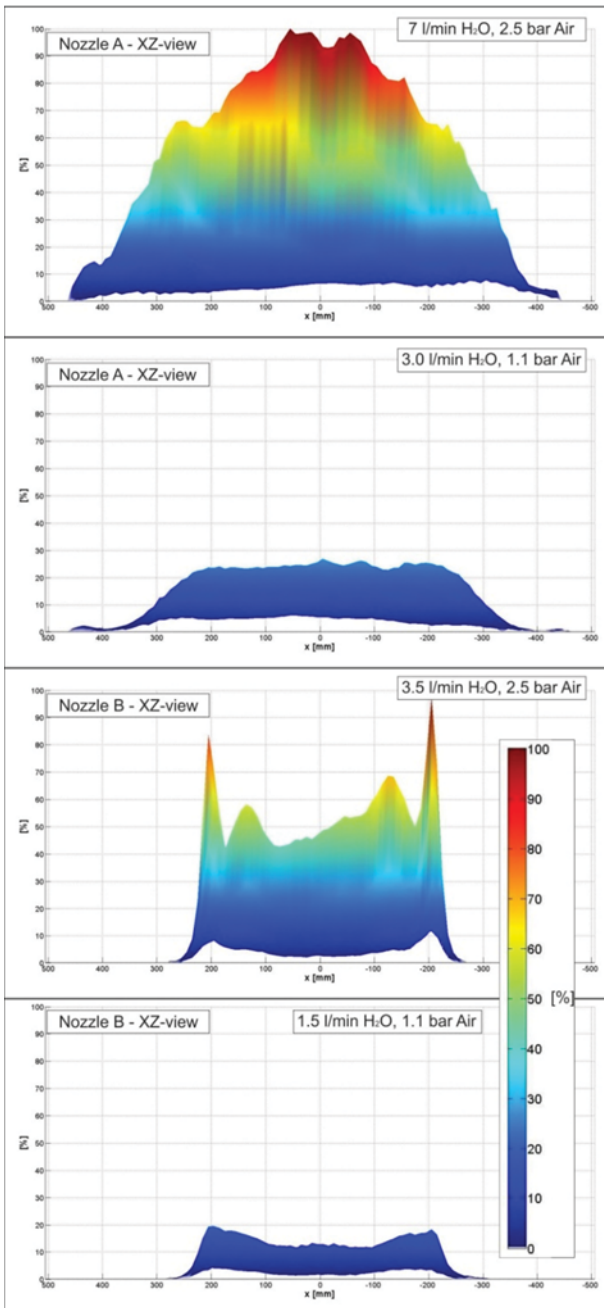
Figure 8: Water distribution of nozzle A and B; XZ "front" view.

Simulation

Measured local heat transfer coefficients at definite positions (Figure 9), case "a" and "b" for both nozzles, were used to describe the heat removal over the spray width (X-direction). Measurements of local HTC were only done for half length of the nozzle due to the clear symmetry of the spray pattern, thus the results were mirrored for the simulation of the plate cooling. Limits to heat removal in spray length (Y-direction) and width were defined according to the water distribution, a HTC value of 200 W/m²K was adjusted for radiation at the remaining regions on the surface. Plate width was fixed as 0.95m with adiabatic boundaries. The thickness of the plate was

set as 40mm with adiabatic regime in the bottom. The plate was moved through the different HTC distributions at a (casting) speed of 0.8 m/min. Simulation results are printed as contour plots with addional color bars for better viewability of the temperature distributions over product width and according to the initial temperature of the steel plate (Figure 10-13).
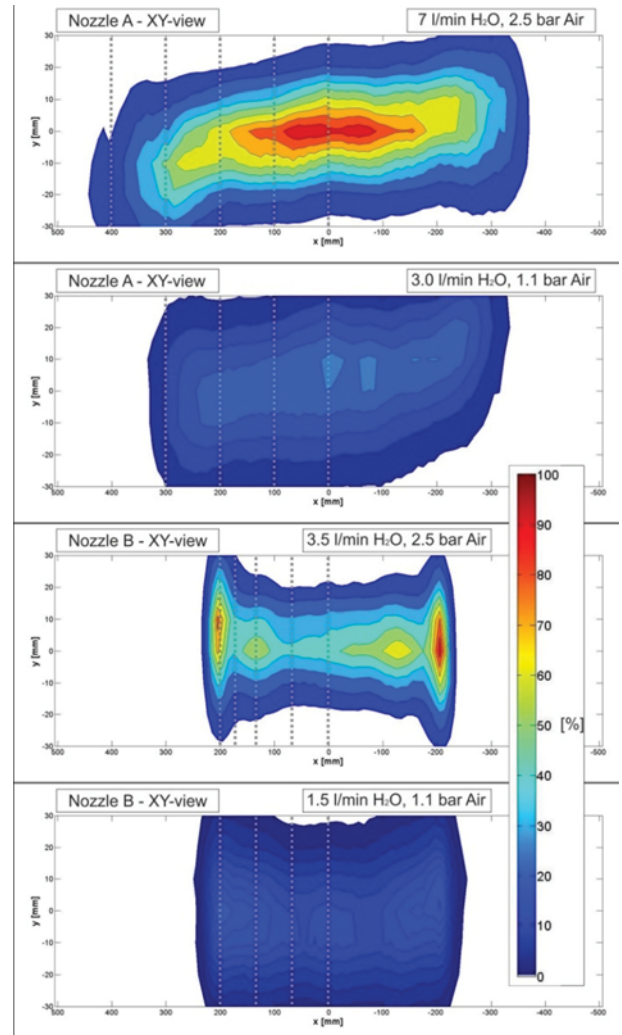

Figure 9: Water distribution of nozzle A and B; XY "topview".

Nozzle A:
Using a minimum amount of water with concurrent low air pressure (case "a") leads to a uniform water distribution over roundabout 400mm spray width (Figure 8, top). The simulation also predicts a nearly uniform heat removal in this region.
Increasing the water impact density (case "b") shifts the distribution to a more pyramidal appearance, leading to a higher heat transfer coefficient in the center of the nozzle with decreasing values towards the edge of the spray width (Figure 8, bottom.)
This first example predicts a higher heat removal when increasing the water impact density, and is in good accordance to the literature.

However, even if the homogeneous water distribution leads to the assumption of a uniform heat removal in the spray width (case "a"), the temperature contour plot in the top of Figure 10 reveals small differences and local temperature drops at the edges of ~10°C that cannot directly explained by the spray water distribution.

In case "b" of nozzle A, the heat transport from the bottom of the plate towards the top leads to a nearly homogeneous temperature distribution on the surface of the plate, after leaving the region of water impact. This example reveals the severity to detect local maxima of heat removal during casting, due to the surface reheating by heat transport from the inner side of the product.

Nevertheless, temperature gradients were present while passing the water distribution, owing to the heat transfer distribution over the spray width. Figure 12 presents snapshots of the temperature distribution at the surface of the plate at Y = 0.176m for all parameter variations. Higher values of the local heat transfer coefficients can lead to temperature differences, reaching a maximum of 32°C for case "b" at $T_{surface,start}$ = 1110°C.
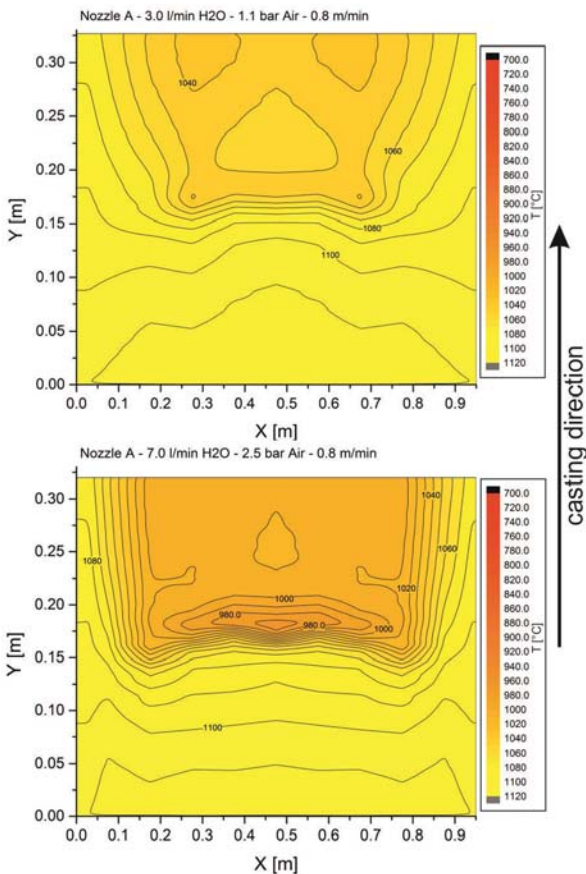

Figure 10: Temperature distribution in case "a" (top) and "b" (bottom), nozzle A, $T_{surface, start}$ 1110°C.

Decreasing the initial surface temperature of the steel plate to 910°C and applying the measured local heat transfer coefficients for that temperature at a casting speed of 0.8m/min, leads to results depicted in

Figure 11. Even if the water impact density was held constant during the tests, while varying only the initial surface temperature, the distribution significantly differs compared to the simulations at 1110°C.

- For low but nearly uniform water impact densities (case "a"), the surface temperature distribution becomes more inhomogeneous.
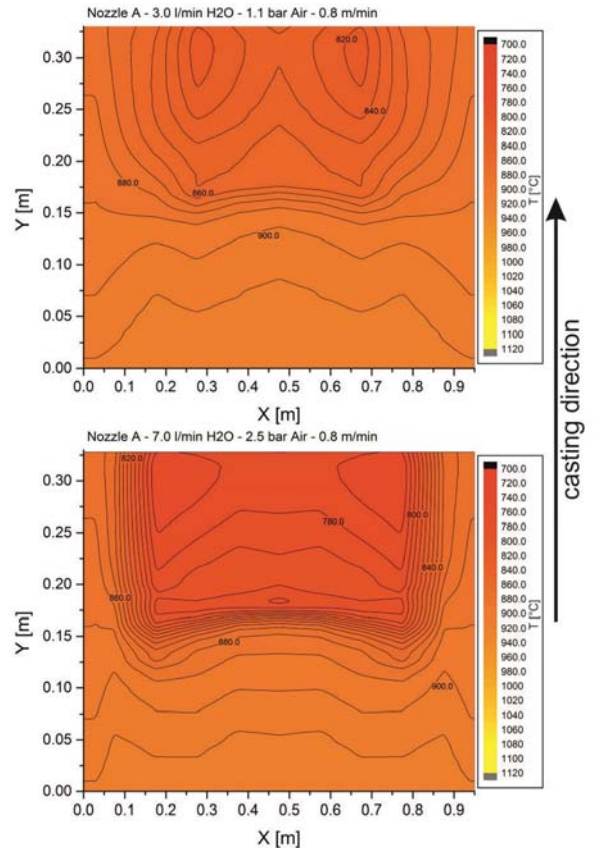- For case "b" a nearly uniform surface temperature can be achieved, in contrast to tests at 1100°C.

Figure 11: Temperature distribution in case "a" (top) and "b" (bottom), nozzle A, $T_{surface, start}$ 910°C.

Taking again a look on the temperature distribution at Y = 0.176m in Figure 12, the more uniform surface temperature over the plate width is clearly visible. Temperature gradients over the spraying width of about 0.6m are below 10°C, decreasing the danger of surface defect formation due to thermal stresses.

Nozzle B:

Independent on the water impact density of nozzle B (case "a" or "b"), two local maxima are present at the edges of the spray pattern, leading to higher local heat transfer coefficients at these positions. Figure 13 and 14 present the contour plots of the simulations, carried out for nozzle B at different temperatures and a constant casting speed of 0.8m/min.
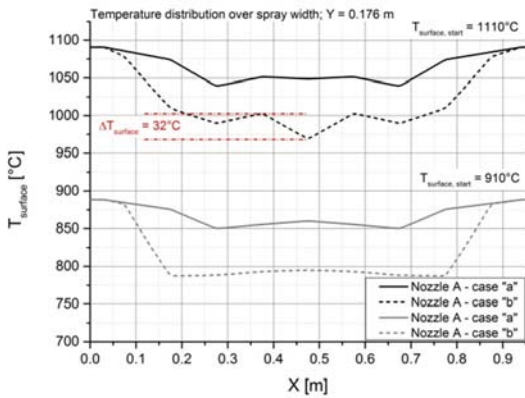
Figure 12: Temperature distribution at position Y = 0.176m for nozzle A.

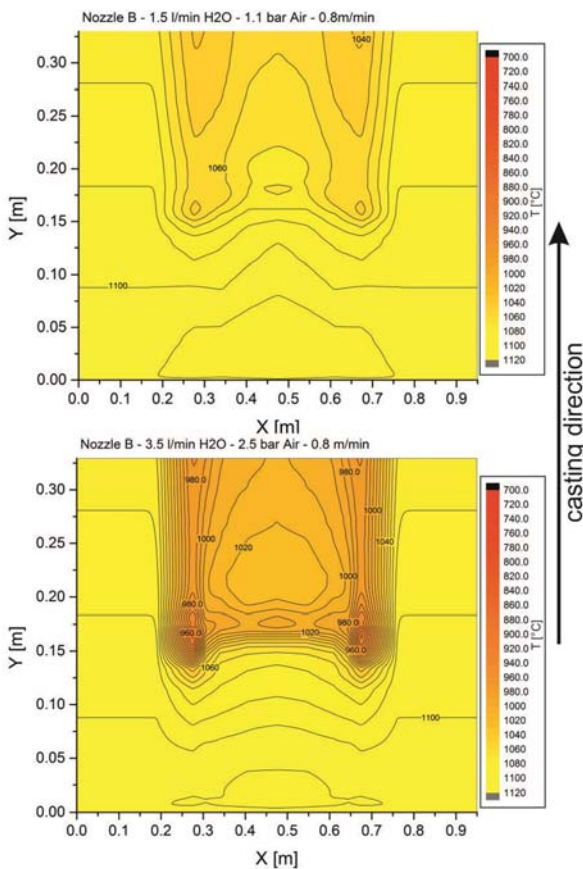*Figure 13: Temperature distribution in case "a" (top) and "b" (bottom), nozzle B, T_surface, start 1110°C.*

At low water impact densities (case "a"), temperature differences already appear at the surface, reaching values of roughly 25°C. High water impact densities (case "b") have a dramatic effect on the heat removal, located mainly on the spray pattern edges and leading to temperature differences up to 91°C (Figure 15).

Heat transport towards the surface from the inside of the plate is not sufficient any more to equalize the temperature distribution, after leaving the area of water impact. Surface defect formation owing to

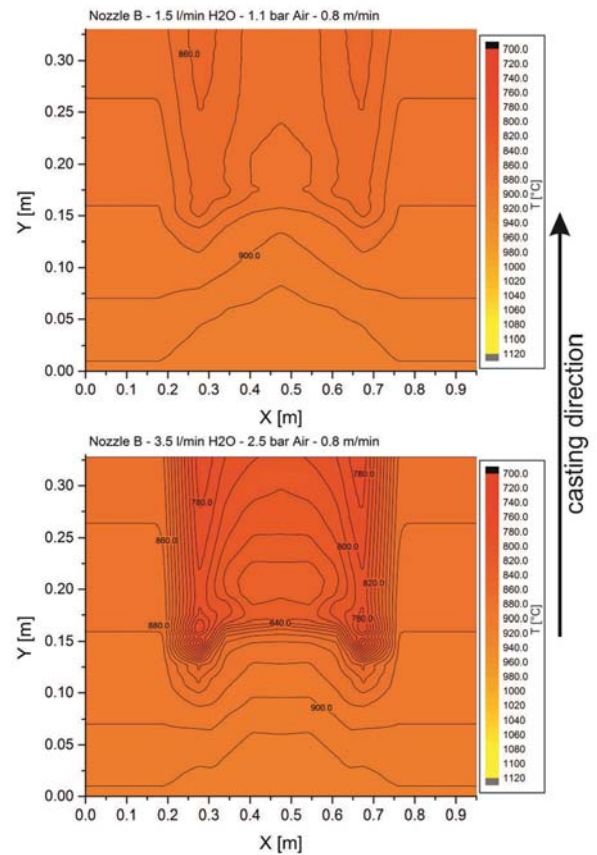thermal stresses in these areas is thus highly probable.

Figure 14: Temperature distribution in case "a" (top) and "b" (bottom), nozzle B, T_surface, start 910°C.

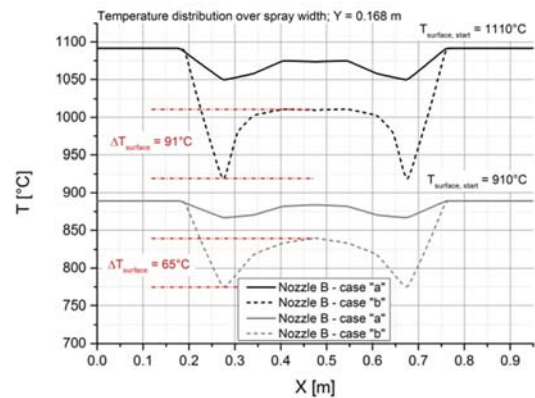*Figure 15: Temperature distribution at position Y = 0.168m for nozzle B.*

Summary

Measurements to determine local heat transfer coefficients were carried out at the Chair of Ferrous Metallurgy, Montanuniversität Leoben, using a so called nozzle measuring stand. Spray parameters of two different nozzles as well as surface temperatures were varied, the determined local HTCs used as input parameter for simulation. A steel plate was moved through the local HTC distribution at a

constant casting speed of 0.8m/min. The results can be summarized as follows:

- Water impact density does not simply correspond to heat transfer coefficient.
- Uniform spray water distributions can lead to inhomogeneous heat withdrawal (nozzle B) and vice versa (nozzle A).
- However, local maxima in water impact density can result in high temperature gradients over spray width, increasing the probability of surface defect formation during casting.
- Detection of local undercooling of the surface may be difficult, if the heat transport from the inside of the product causes a reheating of the surface. Only the surface defects may remain, but the underlying phenomenon is no longer detectable at the end of the casting.

Conclusion

The measurement of local heat transfer coefficients for better characterization of the heat withdrawal during casting is vital. Using a mean value based on water impact density for simulation, in order to keep calculation times low, leads consequently to information losses and makes it difficult to reveal the origins of possible defects in the casted product.

References

[1] Pavlova, A.A., K. Otani and M. Amitay, Active performance enhancement of spray cooling, International Journal of Heat and Fluid Flow 29 (2008), 4, pp. 985–1000.

[2] Puschmann, F., Experimentelle Untersuchung der Spraykühlung zur Qualitätsverbesserung durch definierte Einstellung des Wärmeübergangs, Dissertation, Magdeburg, 2003.

[3] Puschmann, F., E. Specht and J. Schmidt, Local Distribution of the Heat Transfer in Water Spray Quenching, in: K. Ehrke, W. Schneider (Eds.), Continuous Casting, Wiley-VCH Verlag GmbH & Co. KGaA, Weinheim, FRG, 2000, pp. 101–108.

[4] Raudensky, M. and J. Horsky, Secondary cooling in continuous casting and Leidenfrost temperature effects, Ironmaking and Steelmaking 32 (2005), 2, pp. 159–164.

[5] Bendig, L., M. Raudensky and J. Horsky, Spray parameters and heat transfer coefficients of spray nozzles for continuous casting, Conference Proceedings of the 78th Steelmaking Conference, Nashville (1995), pp. 149–158.

[6] Reiners, U., R. Jeschar and R. Scholz, Wärmeübertragung bei der Stranggusskühlung durch Spritzwasser, Steel Research 60 (1989), 10, pp. 442–450.

[7] Hnizdil, M. and M. Raudensky, Influence of water temperature on the cooling intensity during continuous casting and hot rolling, Proceeding of the Metal 2012 Conference, Brno (2012).

[8] Raudensky, M., M. Hnizdil, J.Y. Hwang, S.H. Lee and S.Y. Kim, Influence of Water Temperature on Cooling Intensity of Mist Nozzles in Continuous Casting, In 19th Conference on Materials and Technology, Ljubljana (2011), pp. 60–69.

[9] Bendig, L., M. Raudensky and J. Horsky, Zerstäubungsparameter und Wärmeübertragungseigenschaften einer Zweistoffdüse für die Stranggusskühlung, Proceedings of Spray 94 Conference, Nürnberg, Germany (1994), pp. 1–6.

[10] Stetina, J., F. Kavicka and T. Mauder, Heat transfer coefficients beneath the water cooling nozzles of a billet caster, Proceedings of the Metal 2009 Conference Hradec nad Moravicí, CR, EU (2009).

[11] Wendelstorf, J., K.-H. Spitzer and R. Wendelstorf, Spray water cooling heat transfer at high temperatures and liquid mass fluxes, International Journal of Heat and Mass Transfer 51 (2008), 19-20, pp. 4902–4910.

[12] Reiners, U., R. Jeschar, R. Scholz, D. Zebrowski and W. Reichelt, A measuring method for quick determination of local heat transfer coefficients in spray water cooling within the range of stable film boiling, Steel Research 56 (1985), 5, pp. 239–246.

[13] Wendelstorf, J., R. Wendelstorf and K.-H. Spitzer, Spray Cooling Heat Transfer and Calculation of Water Impact Density for Cooling of Steel Sheet Materials by Inverse Process Modelling, steel research int. 80 (2009), 9, pp. 639–644.